Hydration characteristics assessment of a binary calcium sulfoaluminate-anhydrite cement related with environment temperature

Linglin Xu[1,3] · Chaoyu Tang[1,3] · Haoxin Li[1,3] · Kai Wu[1,3] · Yan Zhang[2] · Zhenghong Yang[1,3]

Abstract

The circumstances in which calcium sulfoaluminate (CSA) cements used are multivariate. Considering the curing temperature greatly influence the formation of hydrates, the hydration of CSA cement containing increasing amount of anhydrite which cured at different temperature was analyzed by calorimetry, XRD and DTA-TGA. And the setting time and mechanical strength are measured to explore the correlation between the microstructure revolution and macroscopic performance. Results illustrate that the hydration of prepared CSA cement is highly dependent on the curing regimes and anhydrite dosage. The addition of anhydrite prolongs the setting of CSA cement at 5 °C, while it accelerates the setting at 20 °C and 40 °C. The usage of anhydrite is detrimental to strength development of CSA cement mortars which cured at 5 °C and 20 °C, but it's the opposite at 40 °C. Additionally, elevated curing temperature favors the formation of ettringite, alumina gel and monosulfate within 1 d. CSA cement prepared with higher amount of anhydrite is beneficially used in the hot environment.

Keywords Calcium sulfoaluminate (CSA) cement · Curing temperature · Hydration · Microstructure · Ettringite

Introduction

CO_2 emission is a serious problem that attracting much more attention of scholar. About 5% of the global anthropogenic CO_2 emissions can be traced to the Portland cement (PC) manufacture [1]. CSA cement as a substitute for PC can reduce such heavy environmental impacts from PC industry, thanks to its lower energy consumption and CO_2 emission during production. Compared with PC, lower sintering temperature and lower electricity energy consumption for grinding in production could reduce CO_2 emission by up to 35% [2–4]. Moreover, the full utilization of by-products, like red mud, slag and even fly ash from municipal solid waste incineration as raw materials in CSA production is realizable [5–8]. Accordingly, CSA cement, especially high belite CSA cement arouses expanding attention from both researchers followed by manufacturers since its invention in 1970s [9, 10].

Hydration of CSA cements highly depends on the amount of the added calcium sulfate and curing temperature. Typically, the CSA cements obtain from market contain 30–70% ye'elimite as a clinker constituent, together with other phases such as belite and calcium aluminates. Those CSA cements with high ye'elimite content (> 50%) are mostly used in combination with Portland cement to manufacture fast-setting, rapid hardening and/or shrinkage compensated construction materials [11], which result from the formation of massive ettringite (AFt). However, two possible problems of AFt-based cementitious materials are (i) their limited thermal stability at or above ~ 100 °C [12]: possibly at lower temperature in low-humidity environment, and (ii) harmful expansion since delayed AFt formation [13]. Elevated temperatures (55 °C and 85 °C) could cause an expeditious transition from AFt to AFm which has been confirmed before [14], accompanying with deleterious dimensional instability and strength reduction [13]. Apart from temperature, anhydrite/ye'elimite molar ratio (M value) also

✉ Haoxin Li
  bosomxin@126.com

1 Key Laboratory of Advanced Civil Engineering Materials (Tongji University), Ministry of Education, 4800 Cao'an Road, Shanghai 201804, People's Republic of China

2 Jianhua Construction Materials Group, Zhenjiang 212413, People's Republic of China

3 School of Materials Science and Engineering, Tongji University, 4800 Cao'an Road, Shanghai 201804, People's Republic of China

affects the decomposition of AFt: at M value of 0.6 or 1.0, AFt starts to dehydrate at 70 °C; whereas when M value was 1.4 or 3.9, AFt kept stable at 70 °C [15].

It has been reported to apply CSA cement in special situations like constructions at low temperature, ocean constructions and rapid repairing for decades [16, 17], where the environmental temperature differs greatly. Numerous literature only investigated the effect of calcium sulfate (mainly with anhydrite or hemihydrate) on the hydration of ye'elimite or CSA clinker at room or elevated temperatures [11, 15, 18–21]. At room temperature, the pure ye'elimite exhibits very slow hydration kinetics during the first 10 h. The addition of calcium sulfate and increasing of pH can accelerate the hydration of CSA cements. Especially the reactivity of calcium sulfate is crucial to control the hydration [15, 20–23]. The amount of the calcium sulfate determines the ratio between the hydration products ettringite, monosulfate and amorphous aluminium hydroxide. Increasing calcium sulfate leads increasing quantity of ettringite and decreasing of monosulfate [11, 21]. Berger et al. [15] cured CSA cements for one week to a thermal treatment simulating the temperature rise (up to 85 °C) and fall occurring in drums of cemented radwastes. The thermal cycle accelerates the early hydration of CSA and reduces the proportion of ettringite versus monosulfate, especially at low gypsum contents. And the thermal cycle reduces the compressive strength and volume stability of gypsum-free CSA cements. The elevated temperature makes the dehydration of ettringite (AFt) to monosulfate and metaettringite under steam curing and dry curing, respectively [18]. According to our previous study, for flue gas desulfurization (FGD) gypsum containing CSA cement, the hydration is highly dependent on the curing temperature (5, 20, 40 °C). Under whichever regime, it's found that more AFt and alumina hydroxide (AH$_3$) generated as the addition of FGD gypsum, while the formation of strätlingite and AFm is inhibited at 40 °C. Therefore, it encourages the strength to develop at 40 °C [24]. However, for current industrial CSA cement manufacture, anhydrite is still the main calcium sulfate resource. Due to the hydration is greatly affected by both anhydrite/CSA clinker ratio and curing temperature, these two factors should be considered at the same time, on the basis of that the single factor has been widely researched before. This paper aimed to study the hydration performance of CSA cement with increasing anhydrite/CSA clinker ratio under different curing regimes. We employed isothermal calorimetry, X-ray diffraction (XRD) and differential thermal analysis-thermogravimetric analyses (DTA-TGA) to determine the heat release of hydration and phase assemblage progression at 5, 20, 40 °C, respectively. Meanwhile, we measured the dimensional stability and compressive strength development of prepared mortars to explore the correlation between the overall performance and microstructure development.

Experimental

Materials and binder formulations

Commercial CSA clinker and anhydrite were used in this present paper. The chemical compositions of CSA clinker were analyzed by X-ray fluorescence (XRF) (Table 1). After analyzing suitable calibration standards, oxide concentrations were computed according to the intensities measured before. Stoichiometric calculations established on XRF analysis and XRD analysis were employed to identify the main mineral composition of CSA clinker, results are also given in Table 1. The densities of clinker and anhydrite are 2.90 g cm^{-3} and 2.87 g cm^{-3}, respectively. Tap water was employed.

The CSA clinkers were prepared as mixtures of commercial CSA and anhydrite in diverse proportion. The replacement amount of anhydrite was 10~50 mass%, indicated with the symbol of A1, A2, A3, A4 and A5. Based on the formation of AFt and AH$_3$ (as shown in Eq. 1), the calcium sulfate demand from undersupply to surplus was covered by the selected range of anhydrite dosage. Reference is the neat CSA clinker which is labeled as A0. The applied water to binder ratio was 0.5. CSA cement mortars were prepared with Chinese standard sand. Per 450 g binder, 1350 g Chinese standard sand was added.
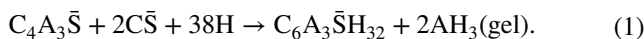
$$C_4A_3\bar{S} + 2C\bar{S} + 38H \rightarrow C_6A_3\bar{S}H_{32} + 2AH_3(gel). \quad (1)$$

Table 1 Chemical and mineralogical compositions of the used materials (mass%)

	XRF analysis		Mineralogical composition	
	CSA clinker	Anhydrite	CSA clinker	
Na$_2$O	0.09	0.04	C$_4$A$_3\bar{S}$	60.28
MgO	1.69	3.00	C$_2$S	23.67
Al$_2$O$_3$	33.36	0.12	C$_4$AF	5.93
SiO$_2$	8.28	1.40	C$_{12}$A$_7$	3.65
P$_2$O$_5$	0.14	–	CT (CaO·TiO$_2$)	2.30
SO$_3$	7.90	50.10		
Cl	0.11	0.02		
K$_2$O	0.23	0.05		
CaO	43.00	44.80		
TiO$_2$	1.35	–		
Gr$_2$O$_3$	0.02	–		
Fe$_2$O$_3$	1.95	0.04		
SrO	0.07	0.44		
ZrO$_2$	0.05	–		
WO$_3$	–	–		
MnO	0.02	–		

Methods

To realize a wide climate temperature coverage, 5, 20 and 40 °C were selected for curing. All the raw materials were kept at the set temperature for 2 days before mixing. Casted cement pastes and mortars were instantly placed under respective temperatures to cure with floating range of ± 1°C, controlling the relative humidity at $60 \pm 10\%$.

Mortars of dimensional 40 mm×40 mm×160 mm were applied to determine the 1, 3 and 28 day compressive strength. The samples were demoulded after 24 h of curing and followed by wrapping with plastic film until arranged ages to resist water evaporation. Ultimately, the compressive strength of every three specimens was tested to calculate the average. Load in the speed of 2.4 kN s^{-1}.

The heat release during hydrating was monitored through isothermal calorimetry at 20 °C and 40 °C. The water to binder ratio was equal to 0.5. Besides the related raw materials, all the glass holders were also placed at respective curing temperature for 2 days before mixing. Samples were internal mixed once contact with water to minimize the external impacts. Measurements were taken within the first 1 d since the fast reaction period of CSA cement.

For XRD and DSC-TGA analysis, a set of samples in shape of cylinder (Ø 35 mm×50 mm) were casted firstly and then crushed at the end of respective curing time. The crushed pastes were soaked into acetone for 7 d to stop hydration. After dried at 40 °C, the samples were kept over silica gel in a desiccator before testing to prevent against H_2O and CO_2. Finally, the samples were ground to powder with particle size not exceeding 70 μm for XRD and DTA-TGA tests.

Main crystalline phases were identified by XRD (Rigaku-D/max2550VB3+) with Cu Kα radiation ($\lambda = 1.541$ Å) at room temperature to record the data, operating the X-ray tube at 40 kV and 100 mA. The scanning range was 2θ of 5–70°, with a step size of 0.02°.

TA Q600 simultaneous thermal analyzer was employed to carry out DTA-TGA measurement. The heating range was 20–1000 °C, with a heating rate of 10 °C min^{-1}. Considering the insensitivity of XRD to amorphous hydrates and poorly crystalline hydrates, in addition to semi-quantitative analysis of AFt (~ 140 °C, based on the assumption that heating 1 mol of AFt lead 20 mol water losing), DTA-TGA was applied to analyse AH_3 through its characteristic dehydration endothermal peak around 280 °C.

Results and discussion

Setting times

The initial and final setting time of all formulations is shown in Fig. 1a, b, respectively. It is very interesting to notice

that the initial setting time of the control (with neat CSA clinker) increases from 151 to 283 min with curing temperature raised from 5 to 40 °C. The retardation of elevated temperature could be ascribed to the increasing amount of AH_3 formed, and such massive alumina gel covers on the unreacted particles [19]. At 5 °C, the setting of samples is prominently prolonged by the addition of anhydrite. For specimen with 50% anhydrite (A5), the initial setting time is prolonged of more than 5 h than A0, which may result from the slow dissolution rate of anhydrite at low temperature [20]. On the contrary, for CSA cement, the decrease of initial setting time is observed instead with increasing amount of anhydrite at 20 °C and 40 °C. For CSA cement with addition of 20% anhydrite, the initial setting time is shortened by 8.8 times to 32 min at 40 °C. When the anhydrite proportion exceed 20%, such acceleration impact of anhydrite is not obvious anymore. Comparing Fig. 1a, b, it can be clearly
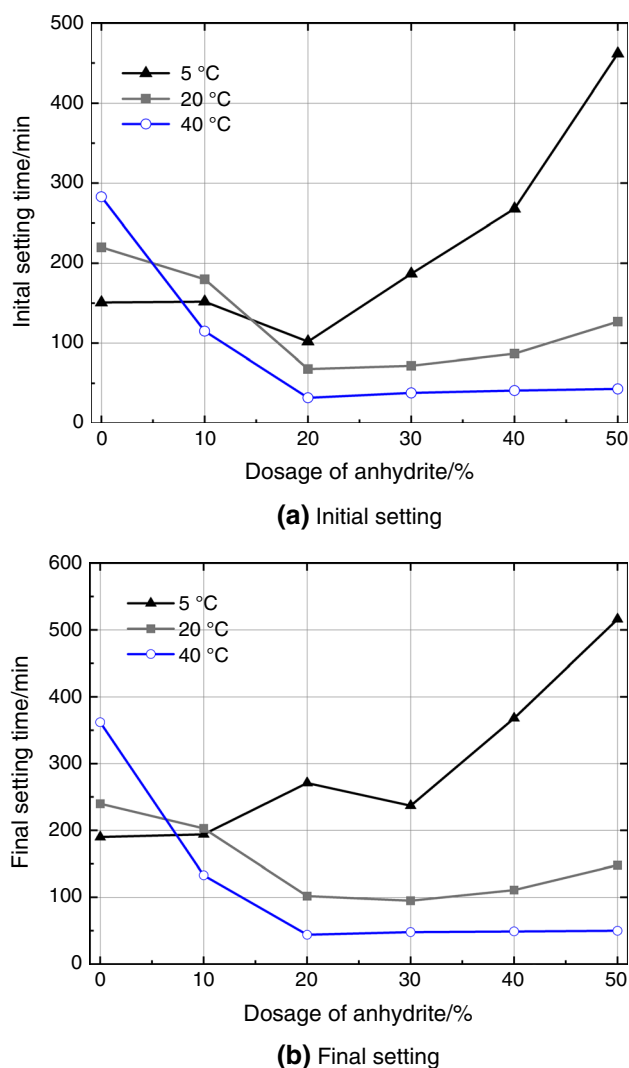

(a) Initial setting

(b) Final setting

Fig. 1 Setting times of CSA cement

noticed that the final setting goes in a similar way with the initial setting.

Compressive strength

The compressive strength of CSA cement mortars cured at different temperature is measured after 1 d and 28 d, respectively (Fig. 2). At 5 °C and 20 °C, the compressive strength of CSA cement mortars tends to decrease prominently and then increases slightly with increasing anhydrite contents. At 5 °C, a replacement of 10% anhydrite leads to a sharp drop of 42 MPa of 1 d-compressive strength. The highest strength is always observed in neat CSA clinker prepared mortar. This is in coherence with previous work [2], the addition of calcium sulfate is not favorable to strength development at ambient temperature. However, all the anhydrite-containing specimens cured at 40 °C exhibit higher strength than the

control sample. The specimen with 20% anhydrite exhibits the highest 1d-strength. For samples cured for 28 days, the compressive strength increases with anhydrite dosage (Fig. 2b). At 40 °C, the 28 d-strength of A5 mortar is about 35% higher than that of A0 mortar.

Hydration heat

The heat evolution rate of CSA cement at different curing temperature is shown in Fig. 3a, b, respectively. It can be clearly seen from Fig. 3a that two main heat releasement steps can be distinguished in the pure CSA clinker (A0) paste which cured at 20 °C. One appears immediately after the water is added into the binder, while the other one appears after 6 h hydration and is followed by an abroad shoulder around 20 h (Fig. 3a). The addition of anhydrite (A2 and A4 pastes), independently of the amount of anhydrite added,
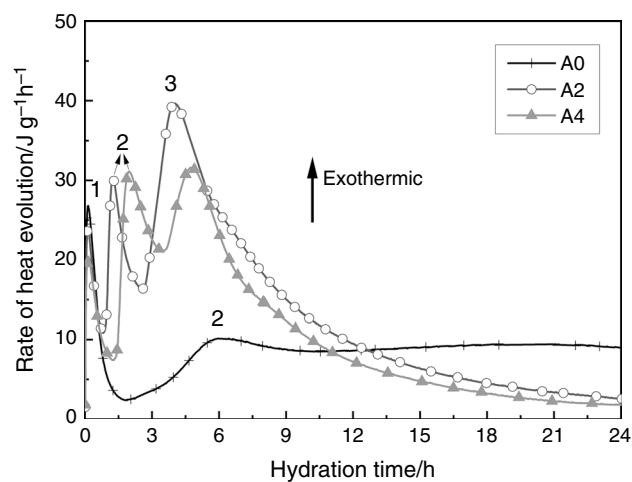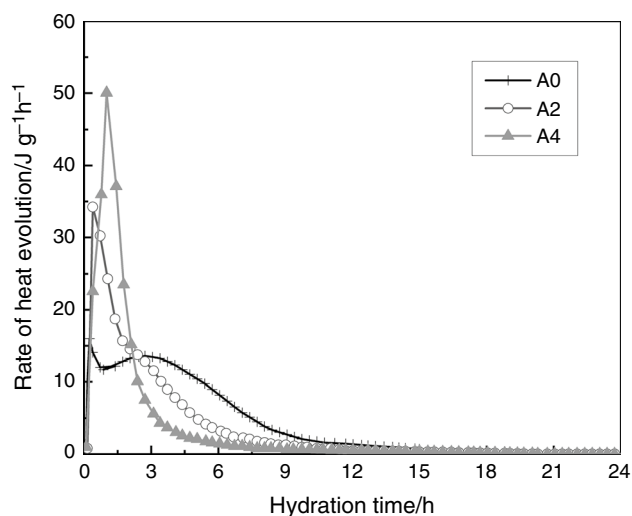

(a) 1 d
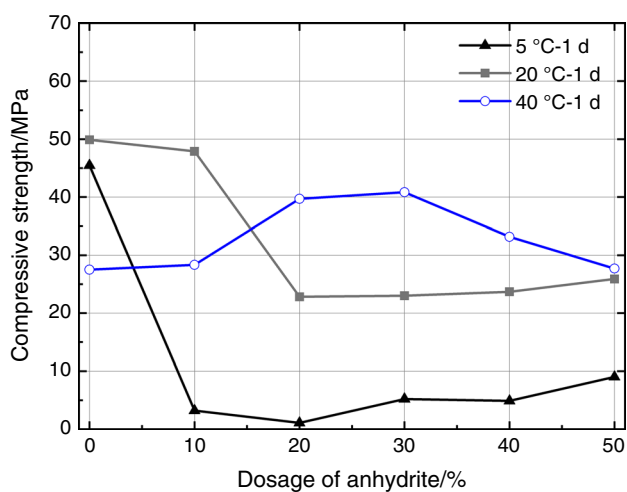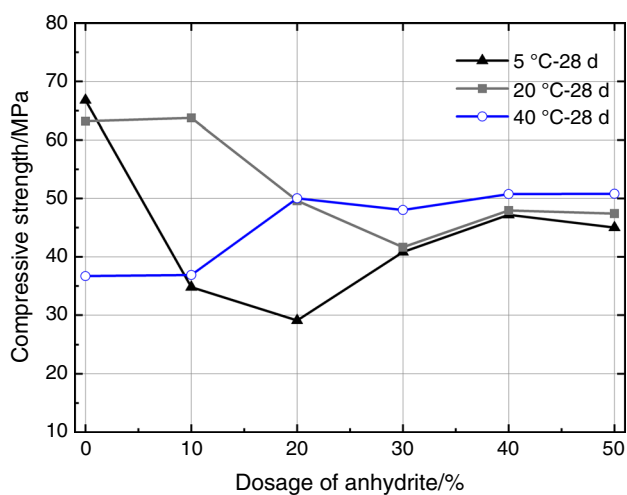
(a) 20 °C

(b) 28 d

(b) 40 °C

Fig. 2 Compressive strength of CSA cement mortars

Fig. 3 Hydration heat of CSA cement

shortens the dormant period. It indicates that the hydration of CSA clinker is accelerated by anhydrite. This finding is in agreement with Ref. [21, 25]. The main part of hydration reactions happens within first 6 h, and three maxima can be distinguished. The first one is attributed to wetting and also the initial formation of AFt. Over this stage, due to the fast dissolution of anhydrite and ye'elimite, the liquid phase becomes saturated with sulfate. Afterwards rapid precipitation of AFt accompanied by the quick consumption of anhydrite, enable the hydration proceeding to stage 2. It is characterized through formation of massive AFt and AH$_3$ at this stage. The quick formation of AFt can be clearly observed in the XRD results, the characteristic peaks of AFt in the XRD pattern of specimen cured for 3 h are much higher than those of 1 h. Nonetheless, since the pore solution is deficient of sulfate, the AFt formed before would convert to monosulfate, and the remaining ye'elimite may hydrate to monosulfate [21, 26]. Eventually, the hydration transits to stage 3. By comparison of A2 and A4 paste, it can be observed that the third heat evolution peak appears behind 4 h and 4.9 h, respectively. This finding indicates that the more anhydrite added, the later stage 3 appears. The rate of heat evolution of stage 2 and 3 decreases with the increasing amount of anhydrite. And after 12 h, once the surfaces of clinkers are covered with hydrates precipitation, the early hydration is hindered.

As for the neat CSA clinker, the induction period associated with dissolution and the very rapid reaction is shortened from 1.5 h at 20 °C to few minutes as the temperature raise to 40 °C (Fig. 3b). This induction period is only followed by one exothermic peak after 3 h, which occurs 3 h earlier than that at 20 °C. After 9 h, early hydration is slowed down. For the anhydrite-containing CSA cement (A2 and A4 pastes), the early hydration is prominently accelerated, together with a more intense heat evolution process. The hydration heat is intensively released in the first 6 h at 40 °C, which is different from that cured at 20 °C and only accounts for half of the time for those pastes at 20 °C.

XRD

Figure 4 presents the XRD patterns of CSA cement pastes cured at different temperature for 0.5 h, 1 h, 3 h and 1 d, respectively. At 5 °C (Fig. 4a), both ye'elimite and belite in A2 and A4 pastes hydrate quite slowly, only trace amount of AFt can be observed within first 3 h. At 20 °C (Fig. 4b) and 40 °C (Fig. 4c), ye'elimite is consumed rapidly, minimal quantity can be detected in those samples cured at 40 °C after 1 d. It is inferred that the consumption rate of ye'elimite increases with the curing temperature. AFt is still the major hydrate, which is the same as that at 5 °C. However, monosulfate (AFm) appears since 0.5 h at 20 °C and 40 °C, and its amount increases gradually with hydration
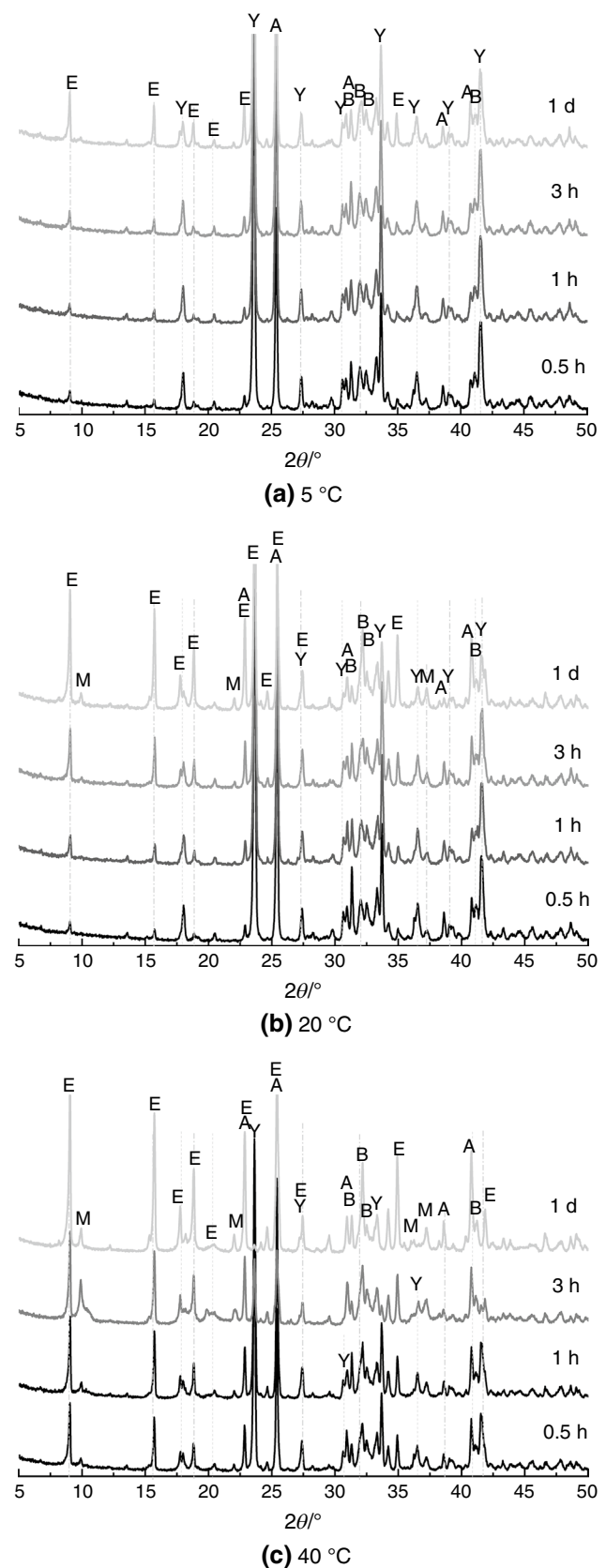

Fig. 4 XRD patterns of A2 paste (with 20% anhydrite) cured at 5, 20, 40 °C (E: ettringite; M: monosulfate; B: belite; Y: ye'elimite; A: anhydrite)

time prolonging. The presence of AFm and anhydrite at the same time indicates that the formation of AFt obeys dissolution–precipitation theory [27, 28], AFm forms once sulfate ion in the pore solution is not available. Since AH_3 and C–S–H are with poor crystallized structure, they are hard to be detected by XRD [29].

Figure 5 shows the XRD pattern of A4 (with undue anhydrite) cured at different regimes. The peak of AFt at around 9.1° becomes stronger with the curing temperature increasing, while the characteristic peak of ye'elimite declines. It is inferred that the kinetic of hydration increase with temperature, similar to A2, which shows no difference with classical Arrehenius Law. AFm phase appears since 1 d at 40 °C (Fig. 5c), which is somehow delayed by the higher amount of anhydrite than A2 paste.

DTA-TGA

As can be observed in Fig. 6a, the amount of AFt decrease and AFm increase with the elevated curing temperature in the paste without anhydrite. And the compressive strength reduction A0 could be caused by the composition change of the hydrates. It is shown in Fig. 6b that the decomposition peak of AFt around 140 °C could be clearly detected at all curing temperatures, and its formation amount tends to increase with temperature, consistent XRD result. Regardless of the curing temperature, AFt is consistently the dominate hydration product (10 mass% at 5 °C, 14 mass% at 20 °C and 21 mass% at 40 °C for 1 d specimens). AH_3 can be clearly identified with a dehydration peak at around 280 °C [30]. As validated by TGA pattern in Fig. 6, elevated temperature favors the formation of AH_3, regardless of quantity of anhydrite added. As shown in Fig. 6c, AFm phases appear simultaneously with AFt at 40 °C in A4 paste.

Discussion

Based on the compressive strength test and the DTA-TGA result, the relationship between 1d-strength of CSA cement and the formation amount of AH_3 and AFt after 1 d is presented in Figs. 7 and 8, respectively. As can be observed in Fig. 7, there is no clear relationship between the formation amount of AH_3 and 1 d-strength. The temperature strongly affects the hydrates of CSA and so that to its compressive strength, but the influence of anhydrite content is relatively weaker. For the specimen with neat CSA clinker (A0), the higher amount of AH_3 which generated at elevated temperature brings to a lower 1d-strength. This finding is totally different with Ref. [31], where it was concluded that the decreasing of amorphous AH_3 content lead to the lower compressive strength ascribing to the generation of AH_3 with huge specific surface area fills empty spaces. Meanwhile, Hu et al. [32] found that the conformation of cracks
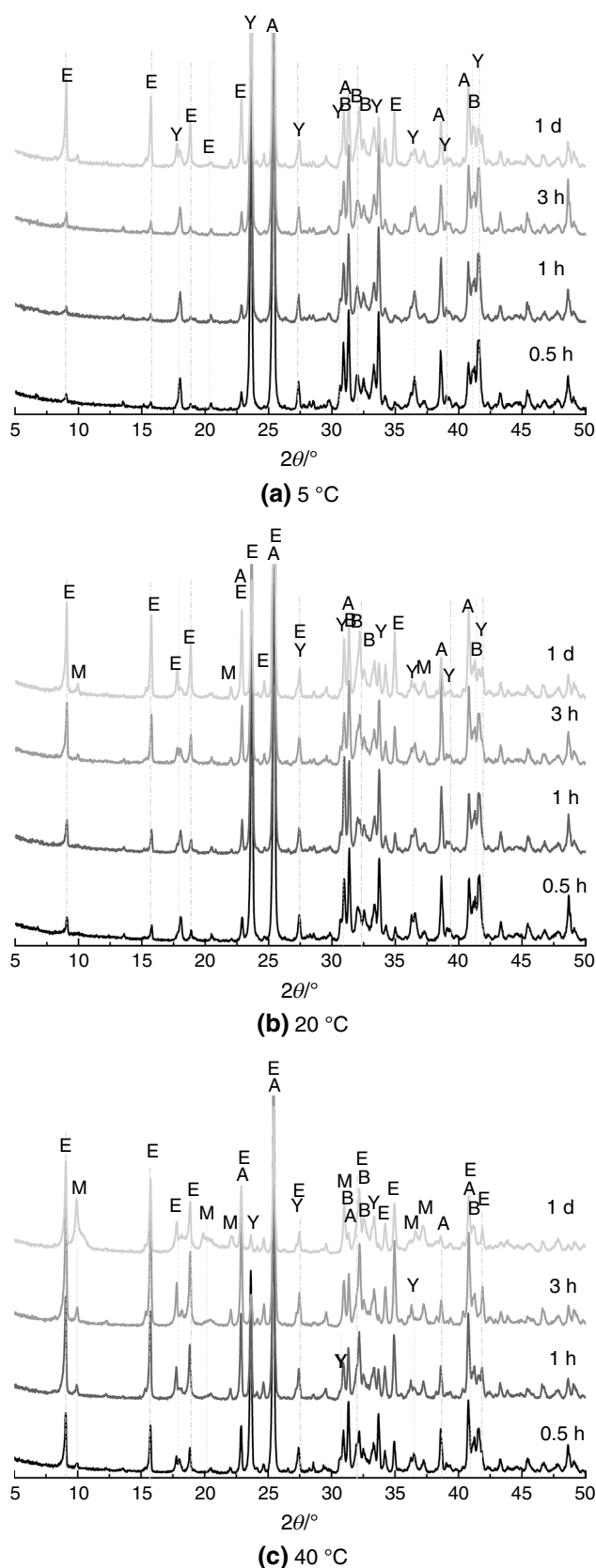

Fig. 5 XRD patterns of A4 paste (with 40% anhydrite) cured at 5, 20, 40 °C (E: ettringite; M: monosulfate; B: belite; Y: ye'elimite; A: anhydrite)

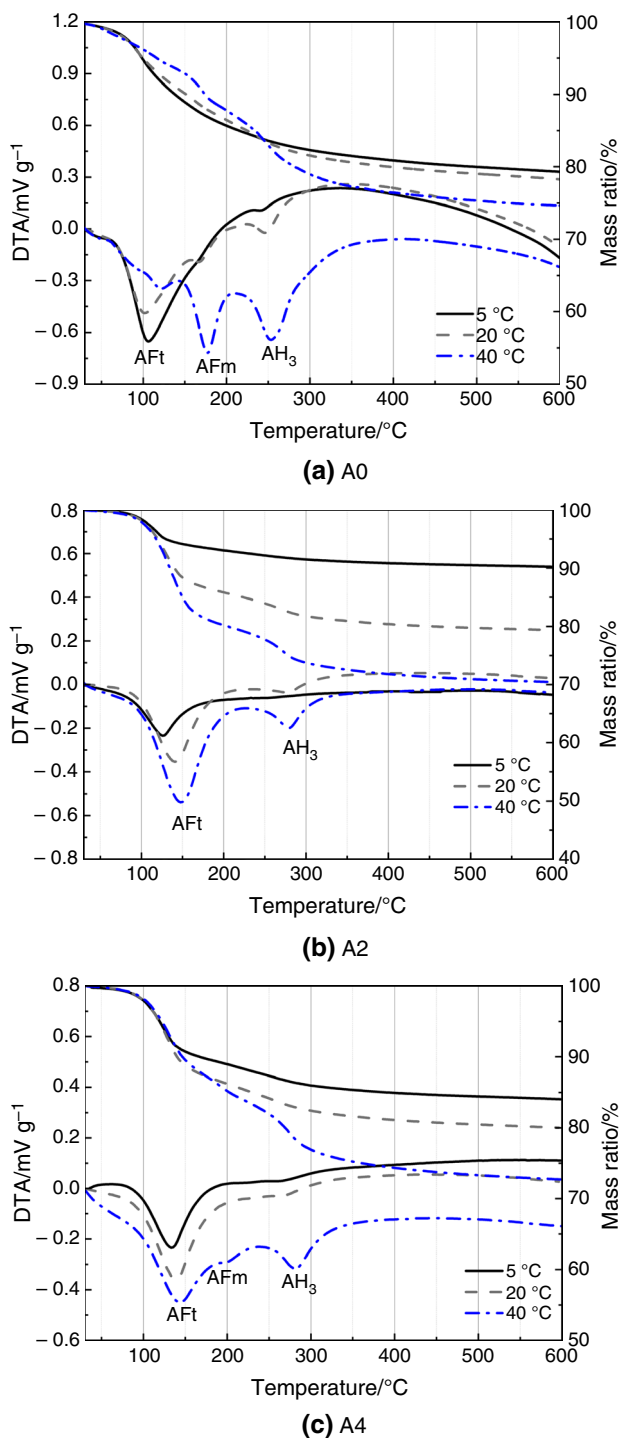**(a)** A0

(b) A2

(c) A4

Fig. 6 DTA-TGA analysis of **a** A0 **b** A2 **c** A4 paste cured at 5, 20, 40 °C for 1 d
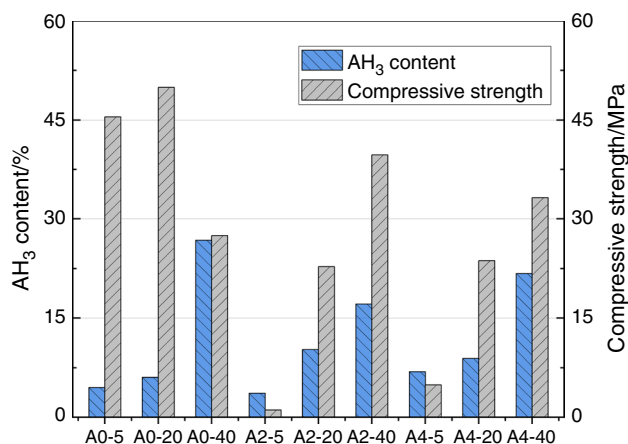

Fig. 7 Comparison of AH_3 content change and compressive strength development
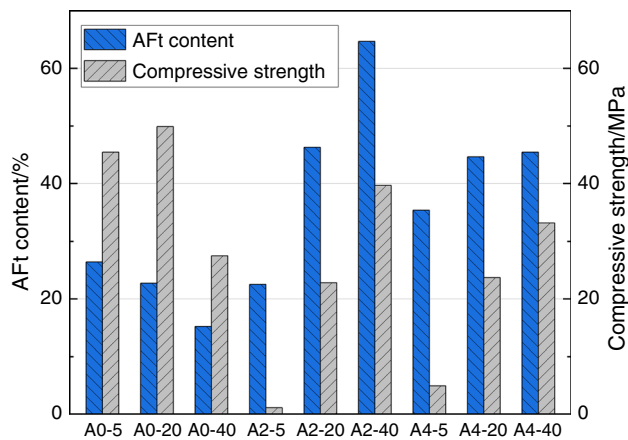
Fig. 8 Comparison of AFt content change and compressive strength development

is greatly influenced by the AFt phase in CSA paste. In CSA clinker paste, pastes containing more AFt exhibited lower indentation modulus and hardness the than the other one which contains more alumina gel at early age. On the contrary, for those anhyd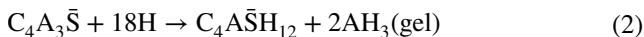rite-containing CSA cement specimens (A2 and A4 pastes), elevated curing temperature favors the formation of AH_3, which accompanied with a higher 1d-strength.

Nevertheless, as can be seen in Fig. 8, 1d-compressive strength is generally in an agreement with AFt formation amount in both CSA clinker and CSA cement pastes. It is quite interesting to notice that after 1 d of curing, AFt is also generated in the paste with pure CSA clinker. The occurrence of AFt confirms that besides the formation of AFm by the hydration of pure ye'elimite (Eq. 2), AFt could be also generated by reaction (Eq. 3) [21, 33]. For those anhydrite-containing specimens (A2 and A4 pastes), elevated temperature favors the formation of AFt, resulting in a higher 1d-strength. On the contrary, less AFt formed in neat CSA clinker (A0) at elevated temperature, leading to a lower 1d-strength. At 40 °C, the highest amount of AFt formed in A2, and this mortar specimen exhibits the highest

compressive strength. The only exception in this figure is that the low AFt amount in the control sample (A0 paste) still contributes to a high 1d-strength.

$$C_4A_3\bar{S} + 18H \rightarrow C_4A\bar{S}H_{12} + 2AH_3(\text{gel}) \qquad (2)$$

$$C_4A_3\bar{S} + 80H \rightarrow C_6A\bar{S}_3H_{32} + C_4A\bar{S}H_{12} + C_3AH_6 + 8AH_3(\text{gel}) \qquad (3)$$
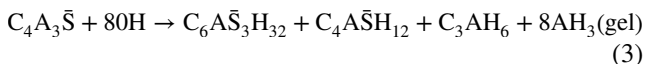
Conclusions

In this work, the anhydrite/CSA clinker ratio and curing temperature are connected to consider whose effects on hydration of CSA cement are studied separately in previous research. At curing temperature of 5, 20 and 40 °C, the hydration features of anhydrite-containing CSA cement were investigated from aspects of compressive strength development, setting times, hydration heat evolution and phase assemblage. The main conclusions are as follows:

(1) Addition of anhydrite decelerates setting of CSA cement at 5 °C significantly, but it accelerates setting at 20 °C and 40 °C. The strengths development of mortars is inhibited by anhydrite at lower curing temperature, while it is favored at 40 °C, especially for later-age strength.

(2) Elevated temperature promotes early hydration prominently, resulting in a more intense heat evolution process for CSA cement pastes and thus a higher rate of heat evolution. Even for the neat CSA clinker paste, the induction period is shortened from 1.5 h to few minutes.

(3) Elevated temperature contributes to a higher amount of AH_3 and AFt in CSA cement pastes, and it also favors the formation of AFm. The 1d- compressive strength of CSA cement has a good agreement with the AFt formation amount. Specimen with 20% anhydrite generates the highest amount of AFt at 40 °C and exhibits the highest 1d- strength.

(4) Comparing the behavior of anhydrite-containing CSA cement to that of neat CSA clinker, the results suggest that anhydrite dosage would normally raise concerns in construction processes when considering climate temperature. At high temperature environment, CSA cement prepared with higher anhydrite content is more suitable.

Declarations

Conflict of interest The authors declare that they have no conflict of interest.

References

1. Habert G. Environmental impact of Portland cement production. In: Pacheco-Torgal F, Jalali S, Labrincha J, John VM, editors. Eco Efficient Concrete. Woodhead Publishing; 2013; https://doi.org/10.1533/9780857098993.1.3.
2. Ioannou S, Reig L, Paine K, Quillin K. Properties of a ternary calcium sulfoaluminate-calcium sulfate-fly ash cement. Cem Concr Res. 2014. https://doi.org/10.1016/j.cemconres.2013.09.015.
3. Berger S, Aouad G, Coumes CCD, Le Bescop P, Damidot D. Leaching of calcium sulfoaluminate cement pastes by water at regulated pH and temperature: Experimental investigation and modeling. Cem Concr Res. 2013. https://doi.org/10.1016/j.cemconres.2013.06.014.
4. Juenger MCG, Winnefeld F, Provis JL, Ideker JH. Advances in alternative cementitious binders. Cem Concr Res. 2011. https://doi.org/10.1016/j.cemconres.2010.11.012.
5. Shen Y, Qian J. Utilisation of phosphogypsum for sulfate-rich belite sulfoaluminate cement production. Adv Cem Res. 2015;27(9):515–25.
6. Mihelj NF, Ukrainczyk N, Leakovic S, Sipusic J. Waste phosphogypsum—toward sustainable reuse in calcium sulfoaluminate cement based building materials. Chem Biochem Eng Q. 2013;27(2):219–26.
7. Wu K, Shi H, Guo X. Utilization of municipal solid waste incineration fly ash for sulfoaluminate cement clinker production. Waste Manag. 2011;31(9):2001–8.
8. Wu K, Hu Y, Zhang L, Su Y, Han J, Yang Z, et al. Quantitative evaluation of interfacial transition zone of sustainable concrete with recycled and steel slag as aggregate. Struct Concr. 2020. https://doi.org/10.1002/suco.202000135.
9. Gartner E. Industrially interesting approaches to "low-CO_2" cements. Cem Concr Res. 2004;34(9):1489–98.
10. Zhang L. Microstructure and performance of calcium sulfoaluminate cements. University of Aberdeen. 2000.https://doi.org/10.1155/2020/7564108.
11. Winnefeld F, Lothenbach B. Phase equilibria in the system $Ca_4Al_6O_{12}SO_4$–Ca_2SiO_4–$CaSO_4$–H_2O referring to the hydration of calcium sulfoaluminate cements. RILEM Tech Lett. 2016. https://doi.org/10.21809/rilemtechlett.2016.5.
12. Zhou Q, Glasser FP. Thermal stability and decomposition mechanisms of ettringite at < 120 °C. Cem Concr Res. 2001;31(9):1333–9.
13. Zhang L, Glasser FP. Hydration products and microstructure of calcium sulfoaluminate cement pastes in different curing regimes. In: Paper presented at the 19th international conference on cement chemistry, Beijing, China, 2015.
14. Zhang L, Glasser F. Hydration of calcium sulfoaluminate cement at less than 24 h. Adv Cem Res. 2002;14(4):141–56.
15. Berger S, Coumes CCD, Bescop PL, Damidot D. Influence of a thermal cycle at early age on the hydration of calcium sulphoaluminate cements with variable gypsum contents. Cem Concr Res. 2011;41:149–60.

16. Ambroise J, Pera J. Use of calcium sulfoaluminate cement to improve strength of mortars at low temperature. Concr Repair Rehabil Retrofit II. 2009;325–6:457.

17. Jen G, Stompinis N, Jones R. Chloride ingress in a belite-calcium sulfoaluminate cement matrix. Cem Concr Res. 2017. https://doi.org/10.1016/j.cemconres.2017.02.013.

18. Kaufmann J, Winnefeld F, Lothenbach B. Stability of ettringite in CSA cement at elevated temperatures. Adv Cem Res. 2015;28(4):251–561.

19. Xu L, Liu S, Li N, et al. Retardation effect of elevated temperature on the setting of calcium sulfoaluminate cement clinker. Constr Build Mater. 2018. https://doi.org/10.1016/j.conbuildmat.2018.05.061.

20. Winnefeld F, Lothenbach B. Hydration of calcium sulfoaluminate cements—experimental findings and thermodynamic modelling. Cem Concr Res. 2010. https://doi.org/10.1016/j.cemconres.2009.08.014.

21. Winnefeld F, Barlag S. Calorimetric and thermogravimetric study on the influence of calcium sulfate on the hydration of ye'elimite. J Therm Anal Calorim. 2010. https://doi.org/10.1007/s10973-009-0582-6.

22. Li H, Xue Z, Liang G, Wu K, Dong B, Wang W. Effect of C-S-Hs-PCE and sodium sulfate on the hydration kinetics and mechanical properties of cement paste. Constr Build Mater. 2021. https://doi.org/10.1016/j.conbuildmat.2020.121096.

23. Sun D, Shi H, Wu K, Miramini S, Li B, Zhang L. Influence of aggregate surface treatment on corrosion resistance of cement composite under chloride attack. Constr Build Mater. 2020. https://doi.org/10.1016/j.conbuildmat.2020.118636.

24. Xu L, Wu K, Li N, Zhou X, Wang P. Utilization of flue gas desulfurization gypsum for producing calcium sulfoaluminate cement. J Clean Prod. 2017. https://doi.org/10.1016/j.jclepro.2017.05.055.

25. Winnefeld F, Barlag S. Influence of calcium sulfate and calcium hydroxide on the hydration of calcium sulfoaluminate clinker. Zkg Int. 2009;12:42–53.

26. Telesca A, Marroccoli M, Pace ML, Tomasulo M, Valenti GL, Monteiro PJM. A hydration study of various calcium sulfoaluminate cements. Cem Concr Compos. 2014. https://doi.org/10.1016/j.cemconcomp.2014.07.002.

27. Georgin JF, Prud'homme E. Hydration modelling of an ettringite-based binder. Cem Concr Res. 2015. https://doi.org/10.1016/j.cemconres.2015.05.009.

28. Perkins RB, Palmer CD. Solubility of ettringite $(Ca_6[Al(OH)_6]_2(SO_4)_3 \cdot 26H2O)$ at 5–75 °C. Geochim Cosmochim Acta. 1999;63(13–14):1969–80.

29. Song F, Yu Z, Yang F, Lu Y, Liu Y. Microstructure of amorphous aluminum hydroxide in belite-calcium sulfoaluminate cement. Cem Concr Res. 2015;71:1–6.

30. Taylor HFW. Cement chemistry. In., 2 edn. Thomas Telford, London, 1997.

31. Chang J, Zhang Y, Shang X, Zhao J, Yu X. Effects of amorphous AH3 phase on mechanical properties and hydration process of $C_4A_3\bar{S}−C\bar{S}H_2−CH−H_2O$ system. Constr Build Mater. 2017.https://doi.org/10.1016/j.conbuildmat.2016.11.111

32. Hu C, Hou D, Li Z. Micro-mechanical properties of calcium sulfoaluminate cement and the correlation with microstructures. Cem Concr Compos. 2017. https://doi.org/10.1016/j.cemconcomp.2017.02.005.

33. Wadsö L. Applications of an eight-channel isothermal conduction calorimeter for cement hydration studies. Cem Int. 2005;3(5):94–101.